Available online at www.eccomasproceedia.org
Eccomas Proceedia COMPDYN (2017) 2805-2822

ECCOMAS
Proceedia

COMPDYN 2017
6th ECCOMAS Thematic Conference on
Computational Methods in Structural Dynamics and Earthquake Engineering
M. Papadrakakis, M. Fragiadakis (eds.)
Rhodes Island, Greece, 15–17 June 2017

SIMPLIFIED ASSESSMENT OF EXPECTED SEISMIC LOSSES FOR AS BUILT AND RETROFITTED RC BUILDINGS

Marco Gaetani d'Aragona[1], Maria Polese[1], Marco Di Ludovico[1] and Andrea Prota[1]

[1] Department of Structures for Engineering and Architecture, University of Naples Federico II
via Claudio 21, 80125 Naples, Italy
{marco.gaetanidaragona, maria.polese, diludovi, andrea.prota}@unina.it

Keywords: seismic losses, retrofit, pushover, Non-linear Response History.

Abstract. *Seismic risk is a key factor influencing several important decision-making processes from performance-based design of new structures, to investments for rehabilitation of existing buildings and even to seismic mitigation campaigns of large building stocks. In order to evaluate the economic convenience of alternative mitigation strategies the expected seismic losses for different solutions (including the "do nothing") in a given timeframe should be compared. The PEER performance-based earthquake engineering framework is normally adopted in order to compute losses. However, its application with a number of Non-linear Response History analyses as a basis for assessment of expected Engineering Demand Parameters and associated losses is an elaborate and time-consuming task, hardly employable for the assessment of earthquake losses for large building portfolios. This paper tests the applicability of a simplified pushover based approach for computation of earthquake losses. Referring to a case study building the results of application of classical PEER approach, i.e. based on Non-linear Response History analyses, are compared with the losses computed with pushover-based assessment, showing encouraging results. In addition, the simplified approach is used to investigate the effect of alternative retrofit strategies on the variation of expected seismic losses.*

Peer-review under responsibility of the organizing committee of COMPDYN 2017.
doi: 10.7712/120117.5608.18010

1 INTRODUCTION

Seismic risk is a key factor influencing several important decision-making processes from performance-based design of new structures, to investments for rehabilitation of existing buildings and even to seismic mitigation campaigns of large building stocks. Within the PEER performance-based earthquake engineering (PBEE) framework [1] the economic losses are adopted as a one of the metrics for measuring seismic risk. In the framework, direct economic losses, that include costs for repairing or replacing damaged buildings, are strongly influenced by the probability of replacement of building (i.e. probability of collapse). Further, if a mitigation action is implemented, the earthquake economic losses are generally reduced, while the costs of building retrofit should be included in the evaluation process [2-5] along with additional metrics in order to account for post-earthquake residual capacity [6,7].
In FEMA P-58 [8], the implementation of the PEER framework is described considering either Non-linear Response History (NLRH) based analyses, either a quicker approach relying on simplified modeling and analysis of the building response that involves the adoption of the SPO2IDA [9] for computation of building fragility.
Starting from the idea of simplifying the computational effort normally required for implementation of the PEER framework, the present paper tests the applicability of standard pushover analysis in combination to the capacity spectrum method, CSM [10] as a basis for the assessment of engineering demand parameters (EDPs) and related damage and losses. The results of detailed evaluation with standard PEER PBEE approach, entailing the execution of a number of Nonlinear Response History (NLRH) analyses and evaluation of EDPs, are compared with results obtained through pushover based assessment of EDPs for a case study non-ductile reinforced concrete (RC) building. In addition, the effect of alternative retrofit strategies is investigated and the variation of expected losses estimated, showing encouraging results on the possibility to adopt pushover-based analyses for estimation of expected costs.
The following section briefly describe the different methods for computation of economic losses. Next, section 3 introduces the reference building, its analytical model, and the design of possible retrofit schemes. Section 4 presents an application of the detailed and simplified assessment for the original building, comparing the results. Finally, the seismic vulnerability reduction as well as the variation of losses are evaluated for adopted retrofit schemes with the simplified approach.

2 EVALUATION OF SEISMIC LOSSES

The PEER PBEE framework, that is probably the most refined procedure currently available, allows quantifying different seismic performance measures such as expected number of injuries or Deaths, economic losses (e.g. expressed in terms of Dollars) and time to recovery or Downtime (the 3Ds). The general approach to loss estimation relies on structural analysis to calculate engineering demand parameters (EDPs) such as deformations and accelerations throughout the structure during an earthquake, which are used to predict the damage in structural, non-structural components, and building contents. Damages are the base for computation of expected losses in terms of one or more of the established metrics (e.g., economic losses in dollars or casualties). The framework operates with four analysis stages: hazard analysis, structural analysis, damage analysis and loss analysis, as synthetically shown in Figure 1.

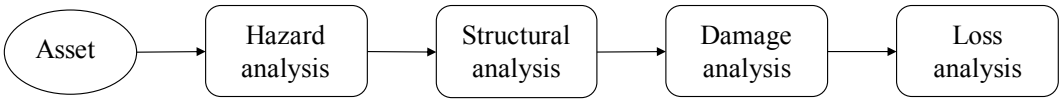

Figure 1. PEER framework [1]

The outcome of each analysis is then integrated using the Total Probability Theorem, allowing to take into account combined numerical integration of all the conditional probabilities and to propagate the uncertainties from one level of analysis to the next, resulting in probabilistic prediction of performance. As noted in [11] the PEER framework is very flexible, since no restrictions are imposed on the approach used to quantify hazard, to perform structural analysis and to relate EDPs to losses and other performance measures. Of course, the results will depend on the assumptions made in applying the procedure and the risk parameters of interest. Different applications of the PEER framework, implementing component-based (e.g. [12,13]) or storey-based damage assessment (e.g. [14]), are available. In this study, a component-based approach is adopted.
In section 2.1 the implementation of the PEER framework proposed by [15] is synthetized, while section 2.2 describes the main differences in the application when pushover based structural analyses for evaluation of EDPs are employed.

2.1 Implementation of the Performance-Assessment Framework for Repair Cost Evaluation

The performance assessment procedure implemented in [15] starts from the identification within the considered facility of the relevant performance groups (PGs), i.e. groups of structural or nonstructural components whose performance is similarly affected by a particular EDP, e.g. acceleration at a given story or IDR_{max} at another story.

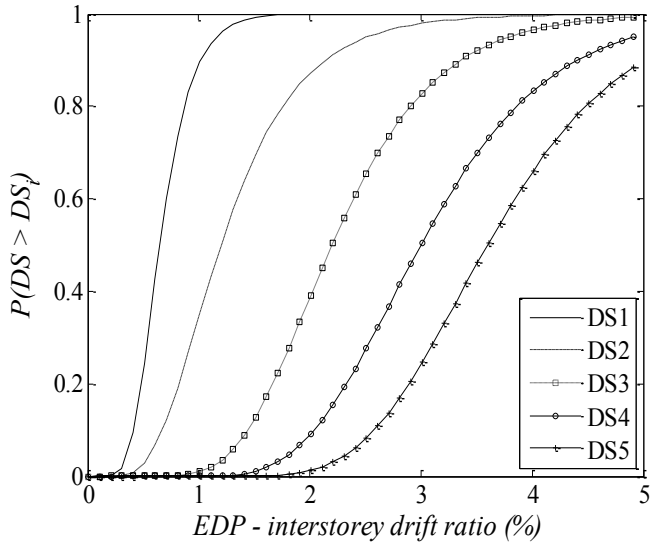

Figure 2. Example of adopted fragility curve

For each PG significant damage states that have a clear correlation with repair actions (and related costs) shall be identified and suitable damage model defined; the latter are expressed in terms of component-level fragility curves, relating EDP (e.g. maximum interstorey drift

ratio, IDR_{max}) to the probability of attaining different damage states for the assigned component type (e.g., Figure 2). In order to allow for quantitative evaluation of the needed repair actions, the number of components or their measurable extension within each PG of the considered facility is estimated.

After selection, e.g. with conventional seismic hazard analysis, of suites of ground motion records, the response of the building is evaluated using NLRH analysis. To allow statistical characterization of EDP at various intensity levels the authors suggest the execution of a number of NLRH analyses with suites of ground motions and for increasing level of hazard. The peak EDP values obtained with NLRH analyses for each record are summarized in an EDP matrix (one matrix for each intensity level); the latter has one column for each considered EDP and one row for each record. Starting from EDP matrices evaluated with structural analysis, additional EDPs are estimated with a simulation-based method that, assuming a joint lognormal distribution among the parameters, enables the generation of large numbers of artificial EDP vectors that have the same statistical distribution as the data that were derived with NRH analyses. This way, large sample of realizations necessary to perform loss evaluations are obtained, and additional sources of uncertainties can be accounted for [8]. The generic EDP realization corresponds to a state of damage. In order to select among possible DSs, given the EDP, a Montecarlo simulation is performed, extracting a random number from the uniform distribution over the interval [0,1]. For example, if the uniform random number generator produces a number of 0.6 and the EDP value shown in Figure 2 is 2.5%, the PG is in DS3.

In this study, 1000 realizations were performed for each intensity level to obtain stable cost estimates. For each realization and PG, a unique damage state was determined. Once the damage state for a performance group is identified, the repair action and the associate repair cost for that performance group is obtained by multiplying cost of new elements by corresponding normalized repair costs by the number of elements in the considered PG. If collapse has not occurred, losses are calculated for each realization based on the damage sustained by each component and the consequence functions assigned to each performance group and by summing repair costs of each PG. If structural collapse was detected, the total repair cost is calculated using the replacement value of the building plus additional costs related to demolition and debris removal. When retrofit strategy is applied, the additional cost due to retrofit intervention is accounted as a repair cost determining a shift to the right of the normalized cost curve.

Finally, considering the repair quantities for each item in the PG, multiplying by a unit repair cost (for each DS) and summing over all items, the total repair cost for the building is computed. To account for possible collapse cases occurred, for each realization an additional Montecarlo simulation is performed based on the collapse fragility curve for the building. For further information about adopted component fragilities and repair costs, refer to [5].

2.2 Simplified assessment employing pushover analysis

A key aspect in the procedure described in 2.1 is the execution of a number of structural analyses performing NLRH with a suite of ground motion records and for different levels of hazard, i.e. for increasing intensity levels. On the other hand, a simpler approach for practitioners is desirable.

Static nonlinear pushover PO, under its applicability hypotheses, allows to investigate a building's nonlinear behavior, assessing damage progression and related variation of displacement profile for increasing levels of seismic demand. Moreover, SPO allows investiga-

tion of damage distribution within the structural system, hence representing a useful tool in the assessment of post-earthquake condition. SPO may be employed for simplified response calculation; by applying the CSM to the capacity curve resulting from pushover analysis [10], the building response to earthquakes of assigned spectral shapes may be found. Scaling the demand spectrum, median expected drift profiles for increasing levels of earthquake intensity can be obtained, hence EDPs in terms of IDR_{max} are determined. Median peak floor acceleration (PFA), can be derived using existing proposals in literature [16-18, 8]. According to FEMA P-58 [8], PFA at floor *i* can be calculated as a function of peak ground acceleration (*PGA)* and an acceleration correction factor H_{ai} (see Equation 1) depending on the strength ratio S, the elastic period of the building T, total building height H and the height above the effective base of the building to floor level *i,* h_i.

$$a_i^* = H_{ai}(S, T, h_i, H) \cdot PGA \qquad \mathrm{i} = 2 \text{ to } \mathrm{N}+1 \tag{1}$$

Statistical distributions of the relevant EDPs (e.g. IDR_{max} of PFA at the different floors) can be derived hypothesizing they have a lognormal distribution and considering the obtained median values (one for each considered intensity level) and suitable dispersions β. By introducing values of dispersion due to modeling uncertainties β_m and inherent randomness associated to earthquake variability, $\beta_{a\Delta}$ or β_{aa} for drift or acceleration respectively, a global value of β may be calculated and EDP probabilistic distribution obtained for each considered intensity level (see e.g. Eq. (2) – valid to assess drift dispersion - and (3)). In Eq. (3) d_{IM} is the median value of drift demand obtained from application of CSM using the demand spectrum scaled at the generic intensity level IM.

$$\beta_{SD} = \sqrt{\beta_{a\Delta}^2 + \beta_m^2} \tag{2}$$

$$P[drift > d \mid IM] = \Phi\left[\frac{1}{\beta} \cdot \ln\left(\frac{d}{\hat{d}_{IM}}\right)\right] \tag{3}$$

Suitable values of β_m and of $\beta_{a\Delta}$ or β_{aa} are suggested in FEMA P-58 as a function of available information for modeling (for β_m) or period and strength ratio S (for $\beta_{a\Delta}$ and β_{aa}).

Once the probabilistic distribution of EDP (e.g. IDR_{max}) at each level of considered intensity are obtained, they can be used similarly to the approach described in 2.1 for computation of expected losses.

3 BUILDING MODEL

The building selected for this study is a seven-story five-bay frame representative of mid-rise non-ductile reinforced concrete building, see Figure 3, "extracted" from the perimeter moment resisting frame of the Van Nuys Holiday Inn located in Los Angeles, California. The concrete nominal strength is f'_c=5 ksi for the first story columns, 4 ksi for the second story columns and second floor beams, and 3 ksi for columns from third story to the seventh and for beams from the third floor to the roof. Column sections is constant along the height and equal to 14"x 20". For further details, refer to [19].

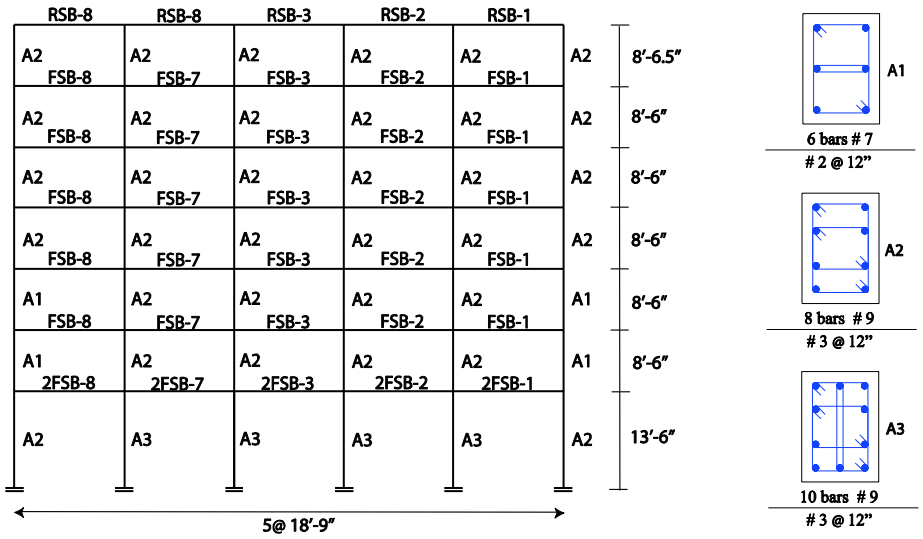

Figure 3. Schematic view of the frame with element number and column rebar arrangement

Similarly, shear and axial failure are expected to occur in non-ductile detailed columns, and consequently shear and axial failure in the columns are explicitly modeled using the Limit State material [20]. P-Δ effects are not included. A schematic view of the building model is shown in Figure 4.

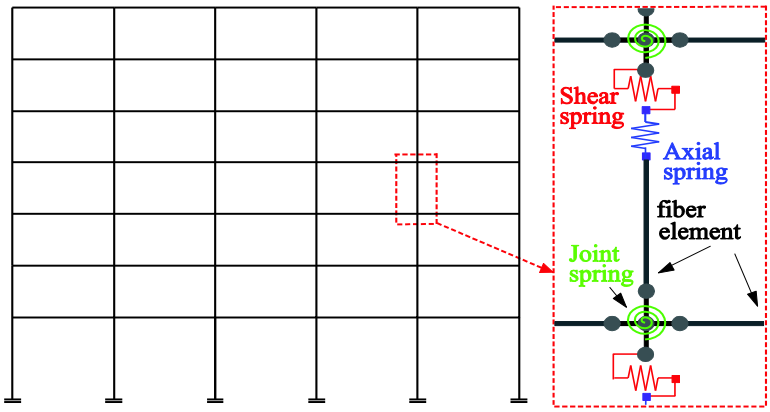

Figure 4. Schematic view of the analytical model

A two-dimensional finite element multi-degree of freedom model developed using [21] is adopted to simulate the seismic response of the building. Beams and columns are modelled using the nonlinear beam-column element [22]. Due to non-ductile details that characterize the structure, is expected that the joints may influence the failure mechanism, consequently the joints are modeled adopting the "scissor model" by [23], including a pinching hysteric behavior [24] to account for the nonlinear shear deformation of the joint.

The eigenvalue analysis of the original structure provides a fundamental vibration period of 1.05 sec. A damping of 2% is assigned to the first and third modes using Rayleigh damping.

To capture the actual capacity for the original non-ductile frame, this study considers two possible system-level collapse mechanisms: Side-sway collapse (SSC) and Gravity load collapse (GLC). The SSC occurs when a single storey has reached its capacity to withstand lat-

eral loads (i.e., when every column in a given floor has reached its residual shear capacity at the same time). GLC occurs when vertical load demand exceeds the total vertical load capacity at a given storey. Collapse is detected based on a comparison of storey-level gravity load demands and capacities (adjusted at each time step to account for member damage and load redistribution). An internal algorithm monitors the dynamically varying capacity of each element and checks the GLC and SSC criteria throughout each nonlinear time history analysis to detect the collapse (with a precision of 0.05g). The collapse is considered as the first between GLC, SSC.

3.1 Retrofit solution with FRP wrapping of selected columns

The first retrofit strategies consist in the application of CFRP layers to enhance the structural performance of RC columns. The wrapping is applied to all columns of selected stories and columns are fully wrapped for their entire height to provide an efficient confinement effect. Column wrapping is designed in order to prevent columns shear failure after yielding.

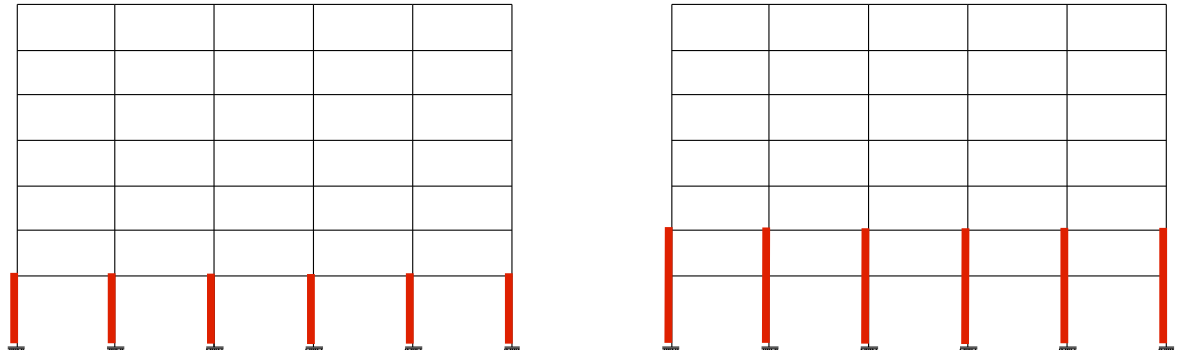

Figure 5. Schematic view of wrapping configuration adopted: (a) wrap1 and (b) wrap12

In particular, the [25] is adopted in the design process in order to provide a shear resistance such that flexural failure is ensured [26]. Two different wrapping configurations are adopted: in the first configuration (*wrap1*) columns at 1st story are fully wrapped (see Fig. 5(a)), while in the second (*wrap12*) columns at 1st and from 2nd story are fully wrapped (see Fig. 5(b)), allowing a higher increment of displacement capacity. For both models, when the wrapping is applied to columns, brittle failure is avoided for all storey columns and their behavior is modeled considering only flexural behavior. The modified behavior of columns materials, due to confining action applied by the CFRP wrapping, is accounted for implementing stress-strain relationship proposed in [27]. When CFRP wrapping is applied, an additional collapse criterion is considered: when in that storey a small increase in ground-shaking intensity causes a large increase in lateral drift response, or when IDR_{max} exceeds the 10% threshold.

3.2 Retrofit solution with insertion of RC wall

The third retrofit strategy consists into adding a RC wall to increase the stiffness and strength of the system. This strategy would have the benefit of reducing the displacement demands but would have the negative effect of increasing acceleration demands.

In particular, the frame is retrofitted by converting the exterior bay to a shear wall composed of a cast-in-place RC panel and boundary columns. The RC panel geometry and reinforcements were designed according to minimum design requirements provided in NIST GCR 11-917-11REV-1 [28].
Analytical model of a coupled wall-frame building system was generated by substituting the right exterior bay with a structural wall modeled adopting the Multiple Vertical Line Element Model (MVLEM) proposed in [29]. The remaining RC frame was connected to the MVLEM implementing rigid diaphragms within each story level. In order to account for the finite size of the shear wall, a rigid beam-column element was adopted within each story level to connect the centerline of the shear wall element with the boundary column at the interface between the frame and the wall.

When the coupled wall-frame strategy is adopted, a substitute collapse criterion is adopted: the system-level collapse is considered attained when the system lateral capacity drops to the 80% of its maximum value.

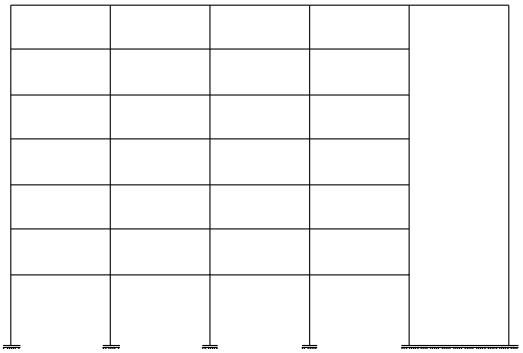

Figure 6. Schematic view of retrofit scheme with shear wall

4 EVALUATION OF EXPECTED LOSSES

4.1 NLRA and cost assessment

Original building

In this section, NLRH analyses are initially adopted to estimate building's collapse capacity through successive scaling until collapse [30] and to estimate building response in terms of EDPs. NLRH analyses are performed for increasing intensities of the seismic action appropriately scaling each record to cover the entire range of structural response, from elastic to ultimate response.

In order to perform NLRH analyses, the set of 30 ground motions adopted in [31] is adopted.

Applying the procedure outlined in 2.1, and considering a total of 1000 realizations for each intensity level to obtain stable cost estimates, total repair costs are obtained.

Figure 7 shows the complementary cumulative distribution function (CCDF) of the total repair cost of the building normalized by building replacement cost (including expected demolition costs), c_r, obtained through the dynamic approach; seven different intensity levels ranging from 0.1g to 0.7g are considered.

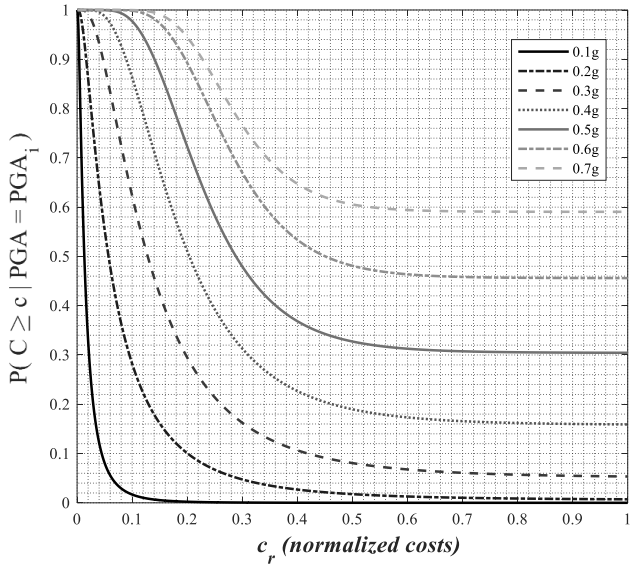

Figure 7. CCDFs of total normalized repair costs (c_r) for different PGAs obtained through NLRH procedure for the original building.

Note that the probability of exceeding a certain level of total normalized repair cost accounting for both the collapse and non-collapse cases is calculated as:

$$P(C_r \geq x) = P(C_r \geq x \mid IM, NC)[1 - P(C \mid IM)] + P(C_r \geq x \mid IM, C)P(C \mid IM) \quad (4)$$

where $P(C_r \geq x \mid IM, NC)$ is the probability conditioned on IM when the structure do not collapses that the normalized repair cost exceeds x; $P(C_r \geq x \mid IM, C)$ is the probability of exceeding the normalized repair cost x given the collapse, that is actually independent from IM and equal to the replacement value of the building; $P(C \mid IM)$ is the probability of collapse conditioned on IM.

Figure 7 shows that with the increase of the damaging action the repair cost inflates making the curve translate rightward, while dispersion of results increases. It is worth to note that the c_r is strongly influenced by the number of collapse cases occurred during the simulation process; consequently, its influence increases as PGA increases (i.e., the probability of collapse increases) making the curve translate upward.

4.2 Simplified assessment via pushover

Original building

In this section, Mass proportional and 1st mode proportional SPO are performed for the original building. Both analyses indicate the activation of a 1st story collapse mechanism, with attainment of gravity load collapse at a roof displacement Δ_{Top} of 0.26 and 0.28 m respectively, corresponding to drifts of 6.24 and 6.84 %.

Figure 8 shows the two pushover curves along with the results of the NLRH analysis, expressed in terms of roof displacement vs base shear, for record Imperial Valley scaled at an

intensity of PGA=0.5g. First story collapse mechanism is attained for 93% of the considered records.

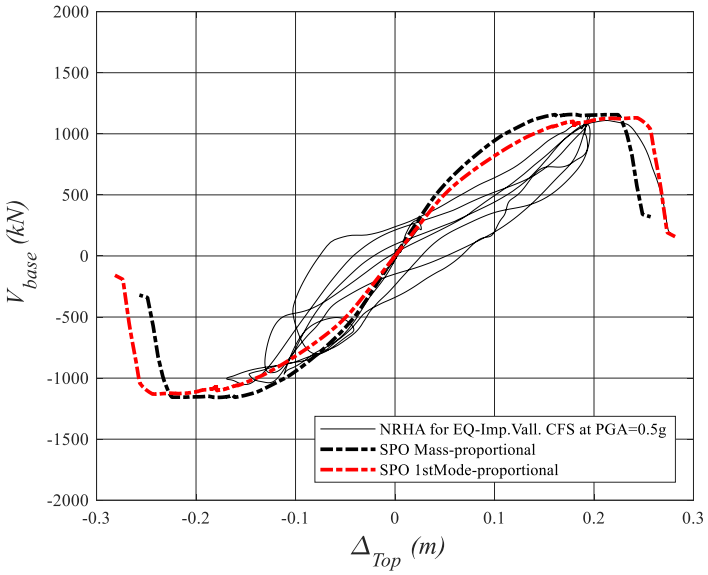

Figure 8. Comparison between Mass and 1st Mode-proportional SPO and NRHA for Imperial Valley 1979 record scaled at PGA=0.5g.

The capacity curves obtained from SPO analyses are transformed in multi-linear curves representing the backbone curve of equivalent SDOF system and IN2 method [32] is applied to compute building capacity and to obtain seismic demand for earthquakes of varying intensity level. The spectrum utilized to apply IN2 method is the mean spectrum of the 30 records utilized for NLRH analyses. Seismic capacity is expressed in terms of peak ground acceleration and indicated as PGA_c(g).

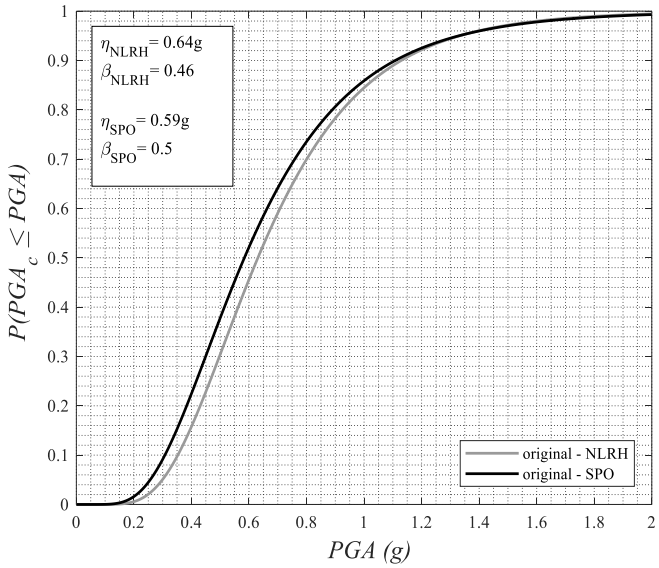

Figure 9. Collapse fragilities for the original building obtained through NLRH and SPO approach.

In particular, the mean result from both SPO analyses is considered, obtaining $PGA_{c,PO}$=0.59g. Median capacity from NLRH analyses is $PGA_{c,NLRH}$=0.64g.

Figure 10 shows the collapse fragility curves obtained from NLRH analyses and with SPO based approach. The latter curve is built considering $PGA_{c,PO}$ as median capacity and the logarithmic dispersion β=0.5, as indicated in [33] for mid-rise old RC frame buildings. It can be noted that the fragility curve representation obtained starting from SPO analyses allows a fair approximation of NLRH-based curve.

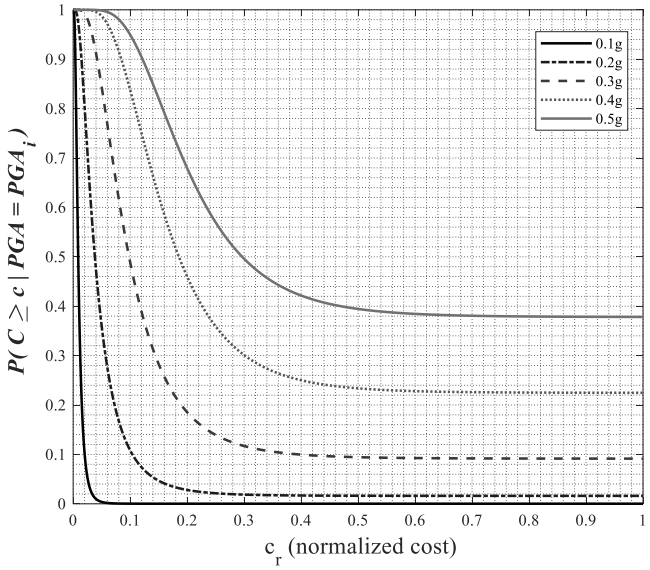

Figure 10. CCDFs of total normalized repair costs (c_r) for different PGAs obtained through SPO procedure for the original building.

In Figure 10, the CCDF of the total normalized repair cost obtained with the SPO approach are depicted. Note that the maximum considered IM corresponds to a_g=0.5 since for higher IMs the SPO considers the structure collapsed. Curves obtained adopting SPO approach show a very similar trend to curves obtained with NLRH. In particular, the SPO-based curves generally underestimate total repair costs for lower intensities, while lead to an overestimation of costs for higher intensities. However, the scatter between detailed and simplified approach is very low. In fact, the higher error between two calculations is attained for PGA=0.1g, where the ratio between the static and the dynamic median c_r, obtained by applying Eq. (4), is about 13%, while the difference between two computations decreases to 5% for 0.3g leading to a slight overestimation when the SPO approach is adopted.

Retrofitted building

Figures 11 and 12 show the SPO curves obtained with Mass-proportional and 1st Mode-proportional load patterns for the three building configurations. As it can be seen, in any cases the retrofit intervention allows an increase of building capacity. In particular, the application of CFRP wrapping increases system ductility not significantly influencing strength, and this effect more sensible in the case of wrap12; while the retrofit scheme that adopts shear wall reduces system ductility while increases system strength. Coherently, the collapse fragility curves obtained using the IN2, shown in Figure 13, evidence a higher shift of the curve of

wrap12 with respect to original building if compared to the shift of wrap1, while the collapse fragility for wall is situated between the two wrap schemes.

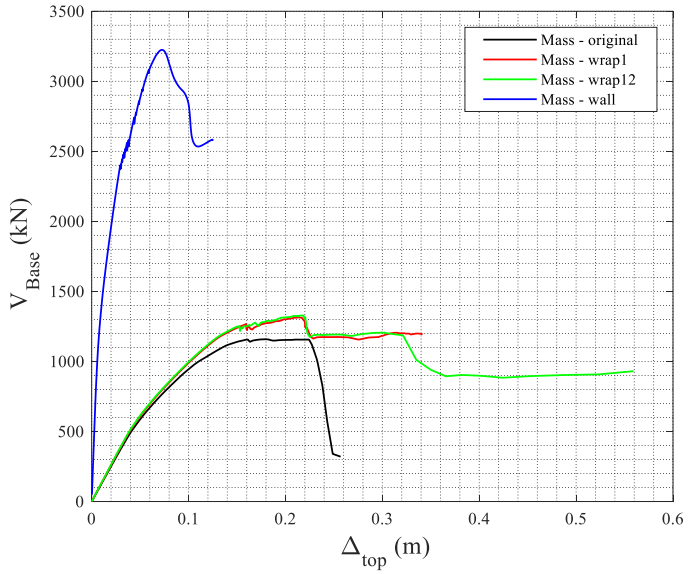

Figure 11. SPO curves obtained with Mass-proportional load pattern for original building and for the three retrofit configurations (wrap1, wrap12, wall)

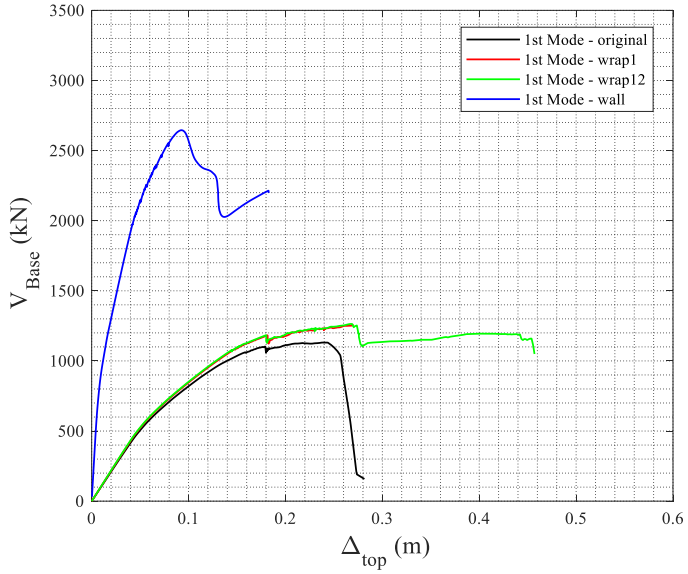

Figure 12. SPO curves obtained with 1st Mode-proportional load pattern for original building and for the three retrofit configurations (wrap1, wrap12, wall)

In fact, as depicted in Figure 13, the median capacity for wrap1 increases from the original value of $PGA_{c,PO}$ =0.58g to $PGA_{c,PO,wrap1}$=0.72g while for the wrap12 and wall configuration it increases up to $PGA_{c,PO,wrap12}$=1.06g and $PGA_{c,PO,wall}$=0.81g. Note that for the retrofit wall that adopts shear wall a logarithmic dispersion β=0.63, as indicated in [33] for mid-rise coupled wall-frame buildings is adopted.

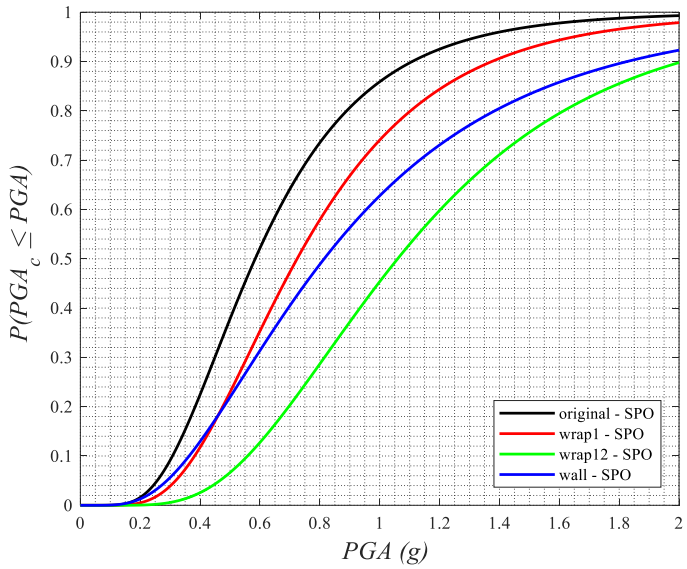

Figure 13. Collapse fragilities for the original building obtained through NLRH and SPO approach and for the three retrofit configurations (wrap1, wrap12, wall) through SPO

Total repair costs are calculated for three building configurations and different earthquake intensities adopting the SPO approach and the procedure outlined in 2.2. For each simulation, the cost of retrofit is added to total repair costs.

Figure 10 shows the CCDFs of the c_r obtained through the SPO approach for three different PGAs and three considered building configurations.

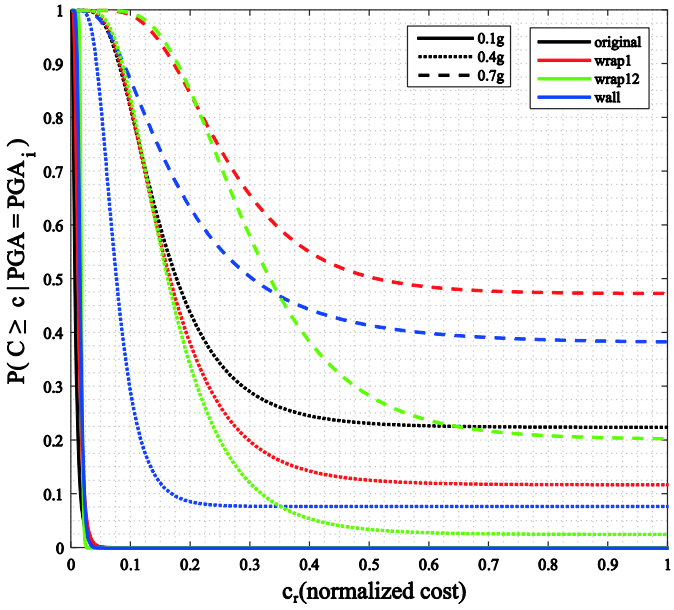

Figure 14. CCDFs of total normalized repair costs (c_r) for different PGAs obtained through SPO procedure

Figure 14 shows that the effectiveness of the retrofit strategy varies depending on the earthquake intensity. In particular, retrofit results to be ineffective for lower intensities where repair costs are mainly ascribable to damage in acceleration-sensitive components while the

influence of collapse probability is negligible. The applied strategies do not significantly modify the peak floor acceleration response of the building, and similar repair costs for four building configurations are expected. As the intensity of ground motion increases, the influence of drift-sensitive components and collapse cases on total repair cost becomes more noticeable. In fact, for a_g=0.4g and for wrap1 and wrap12 the median repair cost decreases of about 6% and 9%, respectively, while for the retrofit scheme introducing shear wall a decrease in repair costs of about 130% is attained due to reduction of drift demand. Further, for higher PGAs, the effectiveness of retrofit in reducing repair costs increases as the collapse capacity increases due to retrofit. For instance, for PGA=0.7g the median value of normalized repair cost drops from 100% (given that structure collapses for $PGA_{c,PO}$=0.59g) for the original building, to 51% for wrap1, 33% for wrap12 and to 30% for wall. Thus, due to the different collapse probabilities when adopting wrap12 and wall schemes, the beneficial effect of the two retrofit strategies becomes similar for higher seismic intensities, when the collapse capacity has the highest influence on repair costs.

5 CONCLUSIONS AND FUTURE STUDIES

The study presented in this paper aims at contributing in the evaluation of the usability of a simplified static pushover (SPO) based approach for the computation of total repair costs.

The efficiency of the SPO approach is demonstrated through an application to a case-study building representative of an existing non-ductile reinforced concrete frame. The response of the frame is simulated using a refined 2D finite element model that properly accounts for possible brittle failures of structural members and captures typical non-ductile RC frames failure modes.

The first comparison in terms of collapse fragility shows that the SPO, coupled to the IN2 method [32], fairly captures the median capacity of the building. In fact, due to the ability of the SPO to capture the most likely collapse mechanism, median capacity evidenced from NLRH is captured by SPO approach with an error of 8%.

Then, the results in terms of total repair costs obtained starting from the classical NLRH approach are compared to those obtained through a SPO-based approach. For both cases, total repair costs are calculated adopting the PEER PBEE framework [1] using a Montecarlo simulation. Additional EDPs are generated using a simulation-based method [15].

In the static approach the IN2 method for increasing earthquake intensities is applied and the EDPs in terms of interstorey drift are calculated. Peak floor accelerations are obtained by simplified formulas [8]. Suitable dispersions are adopted to account for uncertainties not accounted for in SPO.

The results show c_r is strongly influenced by the number of collapse cases occurred during the simulation process; consequently, the incidence of collapse increases as the PGA increases.

The simplified SPO approach shows encouraging results leading to very similar losses obtained through more refined methods when the structure experiences nonlinear deformations, while some improvements are required when the linear range is investigated. In fact, the higher error is attained for PGA=0.1g, where the ratio between the SPO and the NLRH median c_r is of about 13%, while the difference between two methods is lower than 10% for higher PGAs, where the SPO approach leading to a slight overestimation.

These results suggest that, although the results SPO-based procedure will be inevitably affected by a certain degree of approximation with respect to NLRH analyses, the approximated results are justified in the view of a significant reduction of computational burden.

Finally, the SPO approach is implemented considering three possible retrofit schemes adopting complete full-height CFRP wrapping to avoid brittle failures in first (wrap1) and first two storeys (wrap12), and the strengthening of the system through the adoption of a shear wall (wall). In any cases the retrofit intervention allows an increase of median building capacity, that is particularly noticeable for wrap12 (about 80%).

The results of cost analysis show that, the effectiveness of the retrofit schemes vary depending on the earthquake scenario.

In particular, retrofit results to be ineffective for lower intensities where repair costs are mainly ascribable to damage to acceleration-sensitive components while the influence of collapse probability is negligible. The applied strategies do not significantly modify the peak floor acceleration response of the building, and similar repair costs for four building configurations are expected. As the intensity of ground motion increases, the influence of drift-sensitive components and collapse cases on total repair cost becomes noticeable. In fact, for ag=0.4g and for wrap1 and wrap12 the median repair cost decreases of about 6% and 9%, respectively, while for the retrofit scheme introducing shear wall a decrease in repair costs of about 130% is attained due to reduction of drift demand. Further, for higher PGAs, the effectiveness of retrofit in reducing repair costs increases as the collapse capacity increases due to retrofit. For instance, for PGA=0.7g the median value of normalized repair cost drops from 100% for the original building, to 51% for wrap1, 33% for wrap12 and to 30% for wall. Thus, due to the different collapse probabilities when adopting wrap12 and wall schemes, the beneficial effect of the two retrofit strategies becomes similar for higher seismic intensities, when the collapse capacity significantly influences repair costs.

The present study shows that, as expected, the adoption of retrofit strategies increasing ductility capacity does not significantly vary repair costs, except the portion depending on costs related to collapse. Further, it evidences that the adoption of retrofit strategies increasing strength has a slight influence for lower seismic intensities while it significantly reduces repair costs for mid intensities leading to similar effects to those produced by retrofit strategies increasing ductility for higher intensities.

The study does not pretend to be exhaustive, having compared the results of SPO with NLRH for only one case-study frame building.

Additional studies are required to assess the advantages of other alternative strategies in terms of seismic performances, to improve repair cost prediction for low seismic demand and to further simplify the computation of repair costs for an easier application to large building inventories.

ACKNOWLEDGEMENTS

This study was performed within the framework of the PON METROPOLIS "Metodologie e tecnologie integrate e sostenibili per l'adattamento e la sicurezza di sistemi urbani" grant n. PON03PE_00093_4 and the joint program DPC-Reluis 2014-2016 Task 3.3: Reparability limit state and damage cumulated effects. The S.Co.P.E. computing infrastructure at the University of Naples Federico II was used for the parallel computing.

REFERENCES

[1] K.A. Porter. An overview of PEER's performance-based earthquake engineering methodology. In Proceedings of 9th International Conference on Applications of Statistics and Probability in Civil Engineering, 2003.

[2] A.B. Liel, & G.G. Deierlein. Cost-benefit evaluation of seismic risk mitigation alternatives for older concrete frame buildings. Earthquake Spectra, 29(4), 1391-1411, 2013.

[3] M. Polese, M. Marcolini, M. Gaetani d'Aragona, & E. Cosenza. Reconstruction policies: explicitating the link of decisions thresholds to safety level and costs for RC buildings. Bulletin of Earthquake Engineering, 15(2), 759-785, 2017 DOI: 10.1007/s10518-015-9824-0.

[4] M. Gaetani d'Aragona, M.Polese, M. Di Ludovico. Building retrofit prior to damaging earthquakes: reduction of residual capacity and repair costs, paper ID 2490, 16th World conference on Earthquake Engineering, Santiago Chile, January 9th to 13th 2017.

[5] M. Gaetani d'Aragona, M. Polese, A. & Prota. Relationship between the variation of seismic capacity after damaging earthquakes, collapse probability and repair costs: detailed evaluation for a non-ductile building. In 5th ECCOMAS Thematic Conference on Computational Methods in Structural Dynamics and Earthquake Engineering, Crete Island, Greece, 25–27 May 2015 (pp. 1478-1495).

[6] M. Polese, M. Gaetani d'Aragona, A. Prota, & G. Manfredi. Seismic behavior of damaged buildings: a comparison of static and dynamic nonlinear approach, paper #1134, In 4th ECCOMAS Thematic Conference on Computational Methods in Structural Dynamics and Earthquake Engineering, 2013 (pp. 608-625).

[7] M. Gaetani d'Aragona, M. Polese, K.J. Elwood, M. Baradaran Shoraka, & A. Prota. Aftershock collapse fragility curves for non-ductile RC buildings: a scenario ‐ based assessment. Earthquake Engng Struct. Dyn., 2017. doi: 10.1002/eqe.2894.

[8] ATC. 2012. FEMA P-58-1: Seismic Performance Assessment of Buildings. Volume 1– Methodology, 2012.

[9] D. Vamvatsikos, A. Cornell. Direct Estimation of the Seismic Demand and Capacity of Oscillators with Multi-Linear Static Pushovers through IDA. Earthquake Engineering and Structural Dynamics; 35:1097–1117, 2006.

[10] P. Fajfar. Capacity spectrum method based on inelastic demand spectra. Earthquake Engineering and Structural Dynamics; 28:979–93, 1999.

[11] G.M. Calvi, T.J. Sullivan, & D.P. Welch. A seismic performance classification framework to provide increased seismic resilience. In Perspectives on European Earthquake Engineering and Seismology; pp. 361-400, 2014.

[12] H. Aslani, & E. Miranda. Probabilistic Earthquake Loss Estimation and Loss Disaggregation in Buildings, Report No. 157. Stanford, CA: John A. Blume Earthquake Engineering Center, Stanford University, Stanford, 2009.

[13] C.M. Ramirez, A.B. Liel, J. Mitrani-Reiser, C.B. Haselton, A.D. Spear, J. Steiner, ... & E. Miranda. Expected earthquake damage and repair costs in reinforced concrete frame buildings. Earthquake Engineering & Structural Dynamics, 41(11), 1455-1475, 2012.

[14] C.M. Ramirez, E. Miranda. Building-Specific Loss Estimation Methods & Tools for Simplified Performance-Based Earthquake Engineering Report No 171, John A. Blume Eartquake Engineering Research Center, Standford University, Stanford, 2009.

[15] T.Y. Yang, J Moehle, B. Stojadinovic, & A. Der Kiureghian. Seismic performance evaluation of facilities: methodology and implementation. Journal of Structural Engineering, 135(10), 1146-1154, 2009.

[16] C. Petrone, G. Magliulo, & G. Manfredi. Seismic demand on light acceleration‐sensitive nonstructural components in European reinforced concrete buildings. Earthquake Engineering & Structural Dynamics, 44(8), 1203-1217, 2015.

[17] V. Vukobratović, & P. Fajfar. A method for the direct estimation of floor acceleration spectra for elastic and inelastic MDOF structures. Earthquake Engineering & Structural Dynamics, 2016.

[18] T.J Sullivan, P.M. Calvi, & R. Nascimbene. Towards improved floor spectra estimates for seismic design. Earthquakes and Structures, 4(1), 109-132, 2013.

[19] H. Krawinkler. Van Nuys Hotel Building Testbed Report: Exercising Seismic Performance Assessment, PEER 2005/11, University of California, Berkeley, Oct. 2005.

[20] K.J. Elwood. Modelling Failures in Existing Reinforced Concrete Columns. Canadian Journal of Civil Engineering: 846-859, 2004.

[21] OpenSees. Open system for earthquake engineering simulation OpenSees framework-Version 2.5.0. Pacific Earthquake Engineering Research Center, Univ. of California, Berkeley, 2016.

[22] E. Spacone, V. Ciampi, F.C. Filippou. A Beam Element for Seismic Damage Analysis. Report No. UCB/EERC-92/07. Earthquake Engineering Research Center, College of Engineering, University of California, Berkeley, 1992.

[23] S. Alath, S.K. Kunnath. Modeling inelastic shear deformation in RC beam-column joints. Engineering Mechanics Proceedings of 10th Conference, May 21-24, ASCE, Boulder, CO, USA; 822–825, 1995.

[24] W.M. Hassan, J.P. & Moehle. A Cyclic Nonlinear Mac-ro Model for Numerical Simulation of Beam-Column Joints in Existing Concrete Buildings. In Proceedings of the 15th World Conference of Earthquake Engineering, 2012.

[25] ACI 369R-11. Guide for Seismic Rehabilitation of Exist-ing Concrete Frame Buildings and Commentary. Report by ACI committee 369, American Concrete Institute, 2011. ISBN: 978-0-87031-419-3.

[26] ACI 440.2R-08. Guide for the design and construction of externally bonded FRP systems for strengthening concrete structures. Report by ACI Committee 440.2R-08. Farmington Hills, MI, USA: American Concrete Institute, 2008.

[27] M.R. Spoelstra, & G. Monti. FRP-confined concrete model. *Journal of composites for construction*, 3(3), 143-150, 1999.

[28] J.P. Moehle, T. Ghodsi, J.D. Hooper, D.C. Fields, & R. Gedhada. Seismic design of cast-in-place concrete special structural walls and coupling beams: A guide for practicing engineers, NEHRP Seismic Design Technical Brief No. 6, NIST GCR 11-917-11REV-1, Gaithersburg, MD, 2011.

[29] L.M. Massone, K. Orakcal, & Wallace, J.W. Shear-Flexure Interaction for Structural Walls. SP-236, ACI Special Publication – Deformation Capacity and Shear Strength of Reinforced Concrete Members Under Cyclic Loading, editors: Adolfo Matamoros & Kenneth Elwood, 127-150, 2006.

[30] D. Vamvatsikos, A. Cornel.l Incremental dynamic analysis. Earthquake Engng Struct. Dyn. 31 (3), 491-514, 2002.

[31] D. Vamvatsikos, A. Cornell. Seismic Performance, Capacity and Reliability of Structures as Seen Through Incre-mental Dynamic Analysis. Report No 151, John A. Blume Earthquake Engineering Research Center, Stanford University, 2005.

[32] M. Dolsek, & P. Fajfar. Simplified non-linear seismic analysis of infilled reinforced concrete frames. Earthquake engineering & structural dynamics, 34(1), 49-66, 2005.

[33] M. Kosič, P. Fajfar, & M. Dolšek. Approximate seismic risk assessment of building structures with explicit consideration of uncertainties. Earthquake Engineering & Structural Dynamics, 43(10), 1483-1502, 2014.